Optomechanics in an ultrahigh-Q two-dimensional photonic crystal cavity

Amir H. Safavi-Naeini, Thiago P. Mayer Alegre, Martin Winger, et al.

ARTICLES YOU MAY BE INTERESTED IN

Optomechanics in an ultrahigh-*Q* two-dimensional photonic crystal cavity

Amir H. Safavi-Naeini, Thiago P. Mayer Alegre, Martin Winger, and Oskar Painter[a)]
Thomas J. Watson, Sr., Laboratory of Applied Physics, California Institute of Technology, Pasadena, California 91125, USA

We demonstrate an ultrahigh-*Q* slotted two-dimensional photonic crystal cavity capable of obtaining strong interaction between the internal light field and the mechanical motion of the slotted structure. The measured optical quality factor is $Q=1.2\times10^6$ for a cavity with an effective modal volume of $V_{\mathrm{eff}}=0.04(\lambda)^3$. Optical transduction of the thermal motion of the fundamental in-plane mechanical resonance of the structure ($\nu_m=151$ MHz) is performed, from which a zero-point motion optomechanical coupling rate of $g^*/2\pi=320$ kHz is inferred. Dynamical back-action of the optical field on the mechanical motion, resulting in cooling and amplication of the mechanical motion, is also demonstrated. © *2010 American Institute of Physics.* [doi:10.1063/1.3507288]

The strength of the interaction between light and matter, which is fundamental to many applications in nonlinear and quantum optics, depends on the ability to create a large optical energy density, either through increased photon number or photon localization. This may be achieved by creating optical cavities with large quality factors Q and simultaneously small modal volumes V_{eff}. The mode volume V_{eff} in particular can be decreased through the introduction of slots, increasing the electric field intensity in low-index regions of the device. As such, slotted photonic crystal cavities[1] and waveguides[2] have been previously proposed and applied to create highly sensitive detectors of motion[3,4] and molecules.[5] They have also more recently been studied in the context of Purcell enhancement of spontaneous emission from embedded quantum dots.[6]

In the canonical optomechanical system, consisting of a Fabry-Perot resonator with an oscillating end-mirror,[7] the radiation pressure force per cavity photon is given by $\hbar g_{\mathrm{OM}} \equiv \hbar\,\partial\omega_o/\partial x = \hbar\omega_o/L_{\mathrm{OM}}$, where ω_o is the cavity resonance frequency, x is the position of the end mirror, and L_{OM} is approximately equal to the physical length of the cavity. In the quantum realm, one is interested in the zero-point motion coupling rate, which is given by $g=g_{\mathrm{OM}}\sqrt{\hbar/2m_{\mathrm{eff}}\omega_m}$, where m_{eff} is the effective motional mass and ω_m is the mechanical resonance frequency. Large optomechanical coupling, approaching $g_{\mathrm{OM}}=\omega_o/\lambda$, has recently been realized in several different guided wave optical cavity geometries utilizing nanoscale slots.[3,4,8] In this work we design, fabricate, and measure the optomechanical properties of a slotted two-dimensional (2D) photonic crystal cavity formed in a Silicon membrane. Due to the strong optical confinement provided by a sub-100 nm slot and a 2D photonic band gap, this cavity structure is demonstrated to have an optical quality factor $Q>10^6$ and a coupling rate of $g/2\pi=320$ kHz.

A common approach to forming photonic crystal optical circuits is to etch a pattern of holes into a thin dielectric film such as the top Silicon device layer in a Silicon-On-Insulator (SOI) microchip. An effective means of forming resonant cavities in such quasi-2D slab photonic crystal structures is to weakly modulate the properties of a line-defect waveguide.[9–11] Applying this same design principle to slotted

photonic crystal waveguides,[12] optical cavities with $Q\leq5\times10^4$ have been experimentally demonstrated.[5,6] A major source of optical loss in real fabricated structures is light scattering out of the plane of the slab. One class of optical states which play an important role in determining scattering loss are the resonant leaky modes of the slab. These optical resonances are localized to the slab and yet have wave vector components which radiate energy into the surrounding cladding. To reduce the effects of these modes it is preferable to engineer a structure where the photonic crystal waveguide has no leaky mode bands crossing the localized cavity mode frequency. For the popular W1 waveguide[9,10] with a slot added in the waveguide center, we have found that the choice of the slot width is crucial to avoiding coupling to leaky resonances. Figure 1(a) shows the band structure of a slotted W1 waveguide with a hole radius $r=0.285a=134$ nm, slot size $s=0.2a=94$ nm, thickness $t=220$ nm, and nominal lat-
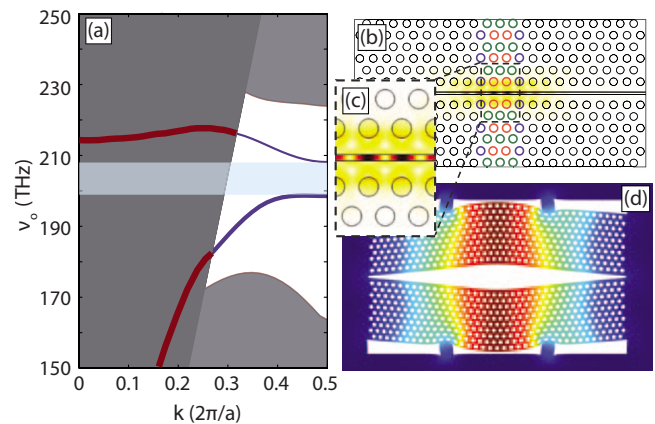

FIG. 1. (Color online) (a) Band diagram for a slotted W1 waveguide formed in a thin ($t=220$ nm) silicon layer. The waveguide slot size is $s=0.2a$, with lattice hole radius $r=0.285a$ for a nominal lattice constant of $a=470$ nm. The light gray shade indicates the guided mode continua, while the dark gray represents the unguided continua of radiation modes. The solid curves are the resonant waveguide bands of the waveguide (the leaky region of the waveguide bands are indicated by a thicker line). The photonic quasiband-gap (for TE-like modes of even vector parity) is highlighted in blue. (b) Electric field intensity, $|\mathbf{E}(\mathbf{r})|^2$ of the optical mode. The defect region of the cavity is indicated by the different colored holes corresponding to different lattice constants. (c) Zoom-in of the slotted region showing strong optical field confinement. (d) Total displacement field $|\mathbf{Q}(\mathbf{r})|$ of the simulated fundamental mechanical mode at 146.1 MHz.

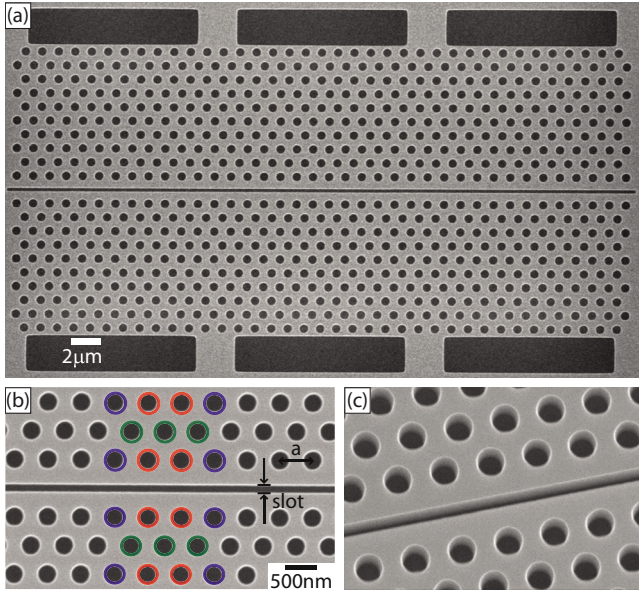a)Electronic mail: opainter@caltech.edu.

FIG. 2. (Color online) (a) SEM image of the fabricated sample. (b) Zoom-in SEM image of the cavity region, with the heterostructure defect cavity region highlighted in false color, and (c) SEM image showing the etched sidewalls of the slot and holes.
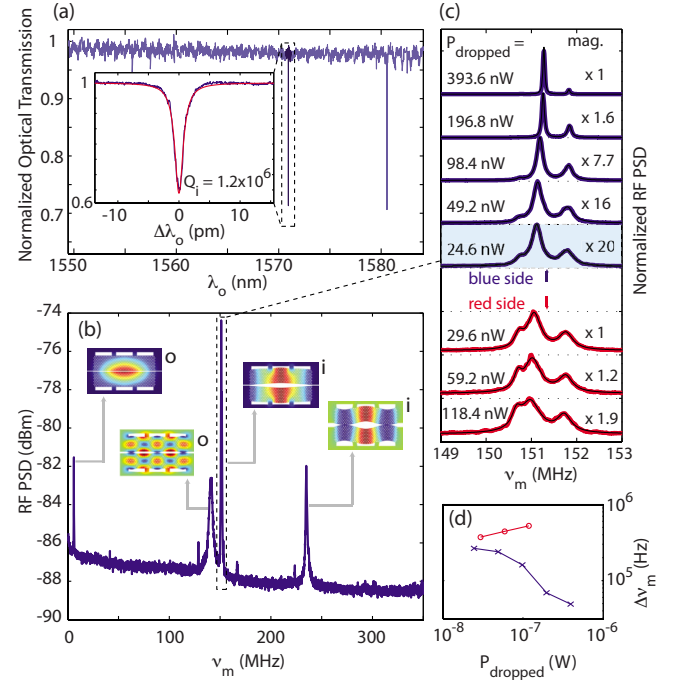

FIG. 3. (Color online) (a) Normalized optical transmission spectrum showing the first and second order optical cavity modes. (inset) Transmission spectrum for the first order mode showing an intrinsic quality factor of $Q_i = 1.2 \times 10^6$. (b) rf-PSD of the photodetected signal, indicating a series of resonance peaks corresponding to mechanical motion of the patterned slab. Insets: FEM-simulated mechanical modes matching the frequency of the strongest few peaks in the spectra ["o" ("i") labels out-of-plane (in-plane) motion]. (c) rf-PSD around the frequency of the fundamental in-plane mechanical resonance for various optical powers dropped into the cavity. The bottom (top) three spectra represent spectrum taken with red (blue) detuning of the input laser from the cavity resonance. Denoted for each spectrum is the optical power dropped into the cavity and a scale factor used to normalize the peak height in each spectrum to a common value. (d) Linewidth of the fundamental in-plane mechanical mode extracted from the spectra in (c). $\times$=blue detuning, o=red detuning.

tice constant of $a=470$ nm. A large band gap for both guided and leaky modes (a "quasibandgap") is clearly present in this structure for the TE-like (even vector parity) modes of the waveguide. On the other hand, for slot widths $s > 0.25a$ the quasibandgap of the waveguide closes due to the presence of leaky resonant bands.

In order to form a localized cavity resonance, we begin with the slotted cavity waveguide structure of Fig. 1(a). A localized resonance is created from the lower frequency waveguide band by reducing smoothly the local lattice constant from a nominal value of $a=470$ nm to a value of $a=450$ nm in the center of the cavity. Three-dimensional finite-element-method (FEM) simulations of the optical and mechanical properties of the resulting cavity structure were performed. The simulated electric field intensity of the fundamental confined optical mode is shown in Fig. 1(b). This mode has a resonance wavelength of $\lambda_o \approx 1550$ nm, a theoretical radiation-limited $Q > 10^6$ and an effective optical mode volume of $V_{eff}=0.04(\lambda_o)^3$.

To allow for mechanical motion of the structure, three rectangular holes of dimensions 4.9×1.0 μm^2 are cut on each side of cavity device as shown in Fig. 1(d). FEM simulations show that this allows for a fundamental in-plane mechanical mode of motion with frequency $\omega_m/2\pi=146.1$ MHz and an effective motional mass of $m_{eff}=20$ pg. The optomechanical coupling between the localized optical and mechanical modes is computed using a variation[13] of the Hellmann-Feynman perturbation theory adopted for optomechanical systems,[14] yielding an optomechanical coupling of $g_{OM}=2\pi \times 480$ GHz/nm, or a zero-point motion rate of $g=2\pi \times 800$ kHz.

Slotted cavities with the dimensions stated above are fabricated using a Silicon-On-Insulator wafer from SOITEC ($\rho=4-20$ Ω cm, device layer thickness $t=220$ nm, buried-oxide layer thickness 2 μm). The cavity geometry is defined by electron beam lithography followed by reactive-ion etching to transfer the pattern through the 220 nm silicon device layer. The cavities are undercut using HF:H$_2$O solution to

remove the buried oxide layer, and cleaned using a piranha/HF cycle.[15] A scanning electron microscope (SEM) micrograph of a final device is shown in Fig. 2(a). Figures 2(b) and 2(c) show the local waveguide defect and slotted region of the cavity, respectively.

The resulting devices are placed in a nitrogen purged box at standard temperature and pressure and characterized optically using a swept-wavelength external-cavity laser ($\lambda=1510-1590$ nm, $\Delta\lambda < 300$ kHz) via a dimpled fiber-taper probe.[16] A broadband cavity transmission spectrum is shown in Fig. 3(a), with the first and second order optical cavity modes separated by roughly by 10 nm, in agreement with simulations. For the first-order mode, optical Q on the order of 10^6 is measured consistently in these devices. A narrow-band optical transmission spectrum (calibrated using a fiber Mach–Zender interferometer) for one such device is shown in the inset of Fig. 3(a), with a measured intrinsic optical $Q_i=1.2 \times 10^6$.

The mechanical properties of the slotted photonic crystal cavity are measured by driving the system with the laser frequency locked to a detuning of a half-linewidth (blue or red) from the cavity resonance. The transmitted cavity laser light is sent through an erbium doped fiber amplifier and then onto a high-speed photodetector. The photodetected signal is sent to an oscilloscope (2 GHz bandwidth) where the electronic power spectral density (PSD) is computed. An ex-

ample of the measured rf-spectrum from a typical slotted cavity device is shown in Fig. 3(b). The fundamental in-plane mode, corresponding to the largest peak in the spectrum, is found to occur at a frequency of $\omega_m/2\pi$ =151 MHz, very close to the simulated value of 146 MHz. rf spectra for various dropped optical powers into the cavity are shown in Fig. 3(c). The corresponding mechanical line-width is plotted in Fig. 3(d). The effects of the retarded component of the dynamical back-action[7] of the light field on the mechanical resonance are clear in both plots, with red (blue) detuning resulting in a reduction (amplification) in the mechanical resonance peak height and a broadening (narrowing) of the mechanical linewidth. One curious aspect of the measured mechanical spectra, however, are the two smaller resonance peaks around the main resonance line. The higher frequency resonance is a result of the splitting of the in-plane differential slab mode into two independent half-slab modes (due to loading by the fiber taper which is placed in partial contact on one side of the slab), while the lower frequency resonance believed to be due to a nearby flexural (out-of-plane) resonances of the slab. FEM simulations show the presence of a flexural mode within a few megahertz of the fundamental in-plane mode, and SEM images show that the membranes are subject to weak stress-induced bowing which can lead to in-plane and out-of-plane mode mixing, resulting in the enhanced optical transduction of the flexural resonance.

The optomechanical coupling of the fundamental in-plane mechanical resonance can be estimated using two different methods. The first method involves calibration of the optical powers and electronic detection system, and uses the fact that the transduced thermal Brownian motion of the mechanical resonator is proportional to g^2.[17] The second method compares the ratio of the rf power in the first and second harmonic of the mechanical frequency. This method is independent of the absolute optical power and detection efficiency, and relies only on accurate knowledge of the optical linewidth. Both of these methods were found to yield an experimental optomechanical coupling rate of $g^* = 2\pi \times 320$ kHz ($g^*_{OM} = 2\pi \times 140$ GHz/nm) for the fundamental in-plane mechanical resonance, roughly a factor of 2.5 times smaller than the FEM-estimated value. As alluded to above, this discrepancy likely results from the splitting of the in-plane motion into two separate slab-halves and the mixing of in-plane motion with the weakly coupled flexural modes of the patterned slab.

In summary, the slotted photonic crystal cavity described here reduces optical scattering loss through the avoidance of resonant leaky modes of the structure while simultaneously allowing for large electric field enhancement in the cavity slot region. The demonstrated optical loss rate of the cavity is $\kappa/2\pi \approx 160$ MHz, which in conjunction with the high mechanical frequency ($\omega_m/2\pi = 151$ MHz) of the fundamental in-plane mechanical resonance, puts this system in the resolved sideband limit of cavity optomechanics ($\kappa/2\omega_m < 1$). The resolved sideband limit is important for a variety of applications, including optical cooling of the mechanical motion to the quantum mechanical ground-state.[18,19] The zero-point motion coupling rate is estimated to be $g^*/2\pi$ =320 kHz for the slotted cavity, due largely to the electric field enhancement in the slot and corresponding to one of the largest values measured to date.[20] The estimated Q/V_{eff} ratio for the measured devices is $3 \times 10^7(\lambda)^{-3}$, indicating that these slotted cavities may also find use in other applications such as Silicon-based cavity-QED (Ref. 6) and sensing.[5]

[1] J. T. Robinson, C. Manolatou, L. Chen, and M. Lipson, Phys. Rev. Lett. **95**, 143901 (2005).

[2] F. Riboli, P. Bettotti, and L. Pavesi, Opt. Express **15**, 11769 (2007).

[3] M. Eichenfield, R. Camacho, J. Chan, K. J. Vahala, and O. Painter, Nature (London) **459**, 550 (2009).

[4] Q. Lin, J. Rosenberg, X. Jiang, K. J. Vahala, and O. Painter, Phys. Rev. Lett. **103**, 103601 (2009).

[5] A. Di Falco, L. O'Faolain, and T. F. Krauss, Appl. Phys. Lett. **94**, 063503 (2009).

[6] J. Gao, J. F. McMillan, M.-C. Wu, J. Zheng, S. Assefa, and C. W. Wong, Appl. Phys. Lett. **96**, 051123 (2010).

[7] T. J. Kippenberg and K. J. Vahala, Science **321**, 1172 (2008).

[8] Y.-G. Roh, T. Tanabe, A. Shinya, H. Taniyama, E. Kuramochi, S. Matsuo, T. Sato, and M. Notomi, Phys. Rev. B **81**, 121101 (2010).

[9] S. G. Johnson, P. R. Villeneuve, S. Fan, and J. D. Joannopoulos, Phys. Rev. B **62**, 8212 (2000).

[10] A. Chutinan and S. Noda, Phys. Rev. B **62**, 4488 (2000).

[11] B.-S. Song, S. Noda, T. Asano, and Y. Akahane, Nature Mater. **4**, 207 (2005).

[12] A. Di Falco, L. Faolain, and T. F. Krauss, Appl. Phys. Lett. **92**, 083501 (2008).

[13] S. G. Johnson, M. Ibanescu, M. A. Skorobogatiy, O. Weisberg, J. D. Joannopoulos, and Y. Fink, Phys. Rev. E **65**, 066611 (2002).

[14] M. Eichenfield, J. Chan, A. H. Safavi-Naeini, K. J. Vahala, and O. Painter, Opt. Express **17**, 20078 (2009).

[15] M. Borselli, T. J. Johnson, and O. Painter, Appl. Phys. Lett. **88**, 131114 (2006).

[16] C. P. Michael, M. Borselli, T. J. Johnson, C. Chrystal, and O. Painter, Opt. Express **15**, 4745 (2007).

[17] M. Eichenfield, J. Chan, R. M. Camacho, K. J. Vahala, and O. Painter, Nature (London) **462**, 78 (2009).

[18] F. Marquardt, J. P. Chen, A. A. Clerk, and S. M. Girvin, Phys. Rev. Lett. **99**, 093902 (2007).

[19] I. Wilson-Rae, N. Nooshi, W. Zwerger, and T. J. Kippenberg, Phys. Rev. Lett. **99**, 093901 (2007).

[20] D. Van Thourhout and J. Roels, Nat. Photonics **4**, 211 (2010).